Ponce, D.A., Hildenbrand, T.G., and Jachens, R.C., 2003, Gravity and magnetic expression of the San Leandro gabbro with implications for the geometry and evolution of the Hayward Fault zone, northern California: Bulletin of the Seismological Society of America, v. 93, no. 1, p. 1-13.

Gravity and Magnetic Expression of the San Leandro Gabbro with Implications for the Geometry and Evolution of the Hayward Fault Zone, Northern California

by D.A. Ponce, T.G. Hildenbrand, and R.C. Jachens

Abstract. The Hayward Fault, one of the most hazardous faults in northern California, trends NNW and extends for about 90 km along the eastern San Francisco Bay region. At numerous locations along its length, distinct and elongate gravity and magnetic anomalies correlate with mapped mafic and ultramafic rocks. The most prominent of these anomalies reflects the 16-km long San Leandro gabbroic block. Inversion of magnetic and gravity data constrained with physical property measurements is used to define the subsurface extent of the San Leandro gabbro body and to speculate on its origin and relationship to the Hayward Fault Zone. Modeling indicates that the San Leandro gabbro body is about 3 km wide, dips about 75-80° northeast, and extends to a depth of at least 6 km. One of the most striking results of the modeling, which was performed independently of seismicity data, is that accurately relocated seismicity is concentrated along the western edge or stratigraphically lower bounding surface of the San Leandro gabbro. The western boundary of the San Leandro gabbro block is the base of an incomplete ophiolite sequence and represented at one time, a low-angle roof thrust related to the tectonic wedging of the Franciscan Complex. After repeated episodes of extension and attenuation, the roof thrust of this tectonic wedge was rotated to near vertical, and in places the strike-slip Hayward Fault probably reactivated or preferentially followed this pre-existing feature. Because earthquakes concentrate near the edge of the San Leandro gabbro but tend to avoid its interior, we qualitatively explore mechanical models to explain how this massive igneous block may influence the distribution of stress. The microseismicity cluster along the western flank of the San Leandro gabbro leads us to suggest that this stressed volume may be the site of future moderate to large earthquakes. Improved understanding of the three-dimensional geometry and physical properties along the Hayward Fault will provide additional constraints on seismic hazard probability, earthquake modeling, and fault interactions that are applicable to other major strike-slip faults around the world.

Introduction

The Hayward Fault, regarded as one of the most hazardous faults in northern California (Working Group on California Earthquake Probabilities, 1999), extends for about 90 km from the Warm Springs District of Fremont in the southeast to San Pablo Bay in the northwest (Fig. 1). Beneath San Pablo Bay the Hayward Fault steps over to the east and continues along the Rogers Creek Fault. The Hayward Fault is a NW trending, predominantly right-lateral strike-slip fault zone that forms the western boundary of the East Bay Hills. About 43 km of right-lateral strike-slip displacement has occurred along the Hayward-Rodgers Creek Faults since about 8 Ma (Fox *et al.*, 1985; McLaughlin *et al.*, 1996). More recently, Wakabayashi (1999a) suggests about 37 to 61 km of late Cenozoic displacement along the Hayward Fault and discusses Holocene and cumulative displacement along the fault. Graymer (2000b) suggests that there may be about 79 km of strike-slip offset on the Hayward Fault Zone based on the restoration of post-12 Ma Miocene volcanic rocks. Active right-lateral slip on the Hayward Fault is evidenced by offset stream channels and man-made features (Lienkaemper *et al.*, 1991), surface geodetic networks (e.g., Lisowski *et al.*, 1991; Linekaemper *et al.*, 1991; 2001), and the 1868 M6.8 earthquake (Bakun, 1999). The Holocene or recent traces of the Hayward Fault (Lienkaemper, 1992) are young features and are only some of possibly many strands in the Hayward Fault Zone, some of which have considerable right-lateral offset (Graymer et al, 1995, Wakabayashi, 1999a; Graymer, 2000b). Herein, the Holocene trace of the Hayward Fault may also be referred to as the recent trace or creeping strand of the Hayward Fault.

A number of on-going and important issues related to the earthquake hazard potential of the San Francisco Bay area remain unresolved (e.g., Simpson, 2000). The Hayward Fault itself is of special interest because the combined earthquake probability of 32% along the Hayward-Rodgers Creek fault system is the greatest in the region (Working Group on California Earthquake Probabilities, 1999). The Hayward Fault is enigmatic in that it both creeps to a depth of about 5 km along its entire length (Lienkaemper. *et al.*, 1991; Savage and Lisowski, 1993) and is capable of producing large earthquakes, evidenced by the October 21, 1868 M6.8 earthquake (Bakun, 1999). However, recent research by Bürgmann *et al.* (2000) utilizing a global positioning system (GPS), interferometric synthetic aperture radar (InSAR), and repeating earthquake clusters indicate that a 20-km portion of the northern Hayward Fault may be creeping throughout the seismogenic zone and thus is less likely to produce a large earthquake. On the other hand, Simpson *et al.* (2001) show that locked patches along the Hayward Fault, inferred from surface creep rates, yield up to 1.7 times as much stored moment than the models of Bürgmann *et al.* (2000), a rate equivalent to a M6.2-6.3 earthquake per century.

The Hayward Fault Zone may be a more important earthquake hazard in the San Francisco Bay area than the San Andreas Fault Zone and may interact and be interconnected at depth with other San Francisco Bay area faults (e.g. Furlong, 1993; Brocher *et al.*, 1994). A seismic reflection study by Parsons (1998) suggests that the Hayward Fault extends into the lower crust and at a depth of 18 km dips 70^{o} to the southwest. The Hayward Fault may also be coupled, in a complex way, to neighboring faults in the San Francisco Bay area, evidenced by a temporary relaxation of creep rates following the 1989 M7.1 Loma Prieta earthquake (Lienkaemper *et al.*, 1997).

Although some of these issues are beyond the scope of this paper, it is because of these emerging and sometimes conflicting findings that a study of the Hayward Fault (Fig. 1) in the vicinity of a gabbro body near San Leandro, a known and quantifiable feature, provides a natural laboratory to advance our knowledge on the geometry and evolution of a major strike-slip fault. Our study deals with the relationship of the active recent trace of the Hayward Fault and the long-term Hayward Fault Zone. Geophysical data along the Hayward Fault are used to investigate the nature and origin of a large gabbro body, hereafter referred to as the San Leandro gabbro. Gravity and magnetic methods are particularly well suited to the study of mafic and ultramafic rocks because of their unusual physical properties. In general, these rocks are strongly magnetic and more dense than

surrounding rocks. In particular, we invert gravity and magnetic data to develop two-dimensional geologic models and to define possible spatial relations between existing and interpreted geologic structures. Existing mechanical models explaining local stress concentrations are explored qualitatively to speculate on the importance of interpreted structures in understanding the hazard of large earthquakes along the Hayward Fault Zone.

Geologic Setting

The study area is separated into two diverse Mesozoic basement terranes by the N35°W-trending Hayward Fault Zone. Franciscan Complex rocks occur on the southwest side of the fault. Coast Range ophiolite plus Great Valley Sequence sedimentary rocks, and presumably wedge-thrusted Franciscan Complex rocks at depth, form the basement on the northeast side of the fault. The Jurassic Coast Range Ophiolite (CRO) consists of gabbro, basalt, keratophyre, diabase, serpentinite, and silica carbonate rocks that are, based on U/Pb isotopic ages of zircons, about 170 to 165 Ma (e.g., Hopson *et al.*, 1981; Mattinson and Hopson, 1992; Hopson *et al.*, 1996). These basement rocks are remnants of oceanic crust (e.g., Bailey *et al.*, 1970; Dickinson *et al.*, 1996; Coleman, 2000) and probably form a dismembered and discontinuous belt along the entire Hayward Fault Zone. Near Hayward (Fig. 1) and near San Lenadro, the San Leandro gabbro body is exposed along the Hayward Fault Zone (Graymer, 2000a).

The Upper Jurassic and Cretaceous Great Valley Sequence (GVS) overlies the CRO and is composed of alternating sequences of sandstone, mudstone, shale, and conglomerate. The GVS consists of clastic submarine fan and basin deposits that were conformably deposited on the CRO (Bailey *et al.*, 1970; Hopson *et al.*, 1981), but this relationship is preserved in only a few places such as one near Hayward and in the Berkeley Hills (Graymer, 1995; Wakabayashi, 1999b). Jurassic and Cretaceous Franciscan rocks are composed predominantly of highly sheared graywacke and argillite; other rocks include shale, large blocks of glaucophane schist, serpentinite, basalt, and chert (e.g., Wakabayashi, 1992; Graymer, 1995).

Cenozoic rocks occur throughout the area, and only a few are older than Miocene age. These marine and non-marine sequences are mostly sandstone, shale, chert, siltstone, conglomerate, volcanic flows, and gravels that rest unconformably on basement rocks (e.g. Graham *et al.*, 1984; Graymer, 1995).

Geophysical and Physical Property Data

Gravity Data

Gravity data (Fig. 2) for the San Francisco Bay region were compiled and supplemented with over 940 new gravity stations adjacent to the Hayward Fault (Ponce, 2001). These data were processed using standard reduction techniques (e.g. Dobrin and Savit, 1988; Blakely, 1995) including topographic corrections to a radial distance of 167 km (Godson and Plouff, 1988) and a combined topographic and isostatic correction to 180° (Jachens and Roberts, 1981). Isostatic corrections were made to remove long-wavelength variations of the gravity field related to local isostatic compensation and are intended to enhance gravity anomalies in the mid to upper crust (Simpson *et al.*, 1986).

Magnetic Data

Two high-resolution aeromagnetic surveys cover the study area. An aeromagnetic survey of Livermore and vicinity (U.S. Geological Survey, 1992) was flown in a N70°E direction, with a flight-line spacing of 500 m (1/3-mi), and a nominal flight-line elevation of 250 m (820 ft) above water and 300 m (1,000 ft) above land. The second survey covers the central San Francisco Bay

area (U.S. Geological Survey, 1996) and was flown in a NE direction with the same flight-line specifications. Both surveys employed precise global positioning navigation systems and data were spaced about 50-m apart along the flight lines. A broad-scale geomagnetic field of the Earth was removed from each survey using the International Geomagnetic Reference Field (Langel, 1992) for the appropriate year of the survey. The aeromagnetic surveys were compiled, merged, and presented as residual total magnetic field anomalies (Fig. 3A).

Physical Property Data

Physical property measurements for selected rock types in the vicinity of the Hayward Fault are shown in table 1. Rock samples and drilled cores indicate that the San Leandro gabbro has a saturated dry bulk density of 2.88 g/cm^3, whereas serpentinite samples along the Hayward Fault have an average density of about 2.54 g/cm^3 (Table 1). Susceptibility measurements show that serpentinite samples along the Hayward Fault Zone are more magnetic than gabbro. The physical properties of the serpentinite samples are similar to those properties described in other studies of ultramafic rocks near the San Andreas fault system that include Red Mountain southeast of the study area (Saad, 1969); Burro Mtn in the Santa Lucia Range, southern California (Burch, 1968; Lienert and Wasilewski, 1979); and along the Sierra Nevada foothills near Mariposa, California (DuBois, 1963). Serpentinization, a low temperature (250-500^{o}C) hydrothermal alteration process, usually produces magnetite as an accessory phase and is accompanied by a decrease in density and an increase in magnetization (e.g. Saad, 1969; Coleman, 1971; Lienert and Wasilewski, 1979).

Interpretive Techniques and Results

The complex gravity and magnetic anomaly patterns shown in Figures 2 and 3 indicate a variety of sources at different depths. Such a superposition of anomalies produced by various sources can result in interpretational ambiguities. The principal goals of a gravity and magnetic study are to detect and quantify changes in mass and magnetic properties at depth and to interpret subsurface geologic structure. Our interpretive approach includes (1) regional magnetic field removal to isolate the anomalies related to near-surface magnetic sources, (2) horizontal gradient analysis to locate lateral changes in magnetization and density, and (3) 2 1/2-dimensional modeling to estimate source geometries and properties.

Regional Magnetic Field Removal

One approach to highlight near-surface geologic boundaries is the removal of a smooth regional field. We first upward continue the magnetic data a small distance (250 m) to approximate the regional magnetic field. Upward continuation tends to remove shorter wavelengths produced by near-surface sources. This regional field was then subtracted from the unfiltered data set to derive a residual field consisting of shorter wavelengths that reflects nearer-surface sources. The resulting residual magnetic data (Fig. 3B) illustrate the effectiveness of this approach to highlight boundaries of subtle magnetic sources that, in this case, are within about 2.5 km of the surface.

An expanded view of the shallow source magnetic map (Fig. 4A) suggests that the San Leandro gabbro body is dissected into at least three slivers, one of which is adjacent to the actively creeping strand of the Hayward Fault (Lienkaemper *et al.*, 1991). Little or no apparent offset of these faulted slivers suggests that there is only minor strike–slip movement on the recently active trace of the Hayward Fault, compared to the total displacement along the Hayward Fault Zone.

East of the Hayward Fault, the shallow source magnetic map (Fig. 3B) reveals an area characterized by a series of linear and low-amplitude magnetic anomalies that reflects a folded and thrusted geologic terrane. Some of these anomalies correlate with the moderately magnetic Neroly Sandstone, along the eastern half of the study area. The Neroly Sandstone is repeated by folding

and faulting in the geologic section (e.g. Graymer, 2000a) and is the primary cause of the striped magnetic pattern northeast of the Hayward Fault.

Boundary Analysis

Potential-field data help to define lateral boundaries and thus can delineate faults or geologic contacts across which density and magnetization differ. Here we apply horizontal gradient analysis to locate such boundaries. Before applying this approach to the magnetic data, we first reduced the magnetic data to the north magnetic pole assuming a total magnetization vector, representative of the study area, with an inclination of 61°N. and declination of 17°E. The reduced-to-the-pole transformation minimizes anomaly asymmetry and approximately centers anomalies over their sources. The reduced-to-the-pole magnetic data are then converted to the magnetic potential, also known as the pseudogravity transformation (Baranov, 1957), which transforms the magnetic field into an equivalent gravity field assuming a density distribution proportional to the magnetization distribution. This transformation is desirable because gravity (or pseudogravity) anomalies have their steepest gradients approximately over the edges of their causative sources, especially for shallow sources, thus the magnetic potential map can be used to approximate the edges of magnetic sources. Maxima in the horizontal gradients of the gravity field or the magnetic potential occur near steep boundaries separating contrasting densities or magnetizations. The locations of these maximum horizontal gradients were determined using a method described by Blakely and Simpson (1986), and linear features interpreted from them are shown in Figure 4B.

This boundary analysis defines a structural block, the San Leandro block, which is delimited by the thick red and blue lines on Figure 4B. The eastern boundary of this geophysically defined structural block is coincident with the mapped Chabot fault. The westernmost boundary of the block is west of the recent trace of the Hayward Fault and west of the westernmost surface exposures of the San Leandro gabbro by about 1 km. This westernmost boundary reflects the buried horizontal extent of the dense and moderately magnetic San Leandro gabbro body. In general, other linear features derived from the maximum horizontal gradients of the gravity and magnetic potential data, reflect faults or abrupt changes in physical properties, such as the edge of the moderately magnetic Neroly Sandstone (Tn, Fig. 4B) northeast of the Hayward Fault.

Two-dimensional Models

We used a 2 1/2-dimensional simultaneous gravity and magnetic modeling program called GMSYS (names of private products are for descriptive purposes only and do not imply endorsement by the U.S. Geological Survey), which is a mouse-driven and more elaborate version of SAKI (Webring, 1985), based on generalized inverse theory. The program requires an initial estimate of model parameters (depth, shape, magnetization, and density of suspected sources) and then varies selected parameters in an attempt to reduce the weighted root-mean-square error between the observed and calculated potential fields. Three gravity and magnetic models (Fig. 5) were constructed across the San Leandro gabbro essentially perpendicular to the trend of the Hayward Fault and surrounding structural trends (Fig. 1). The northernmost profile transects the maximum magnetic anomaly associated with the San Leandro gabbro (Fig. 3A) whereas the central profile transects the maximum gravity anomaly (Fig. 2) associated with the San Leandro gabbro.

The interpretation of potential-field data yields non-unique solutions because an infinite number of geometrical models will have an associated field that closely matches the measured field. For example, increasing the magnetization while decreasing the thickness of a proposed gabbro body, will generally not produce an appreciable change in the computed field. Although, potential-field modeling is non-unique, the final models are based on numerous iterations and have been extensively tested to produce a model that is geologically reasonable with minimum structural complexities. The synthesis of the potential-field data and independent constraints described below,

leads to a family of similar models, regardless of the starting model, with characteristics that support our major conclusions on the subsurface geology.

The geophysical models are constrained by physical property measurements on hand-sized and drill-core samples from selected rock types, some of which are shown in table 1. Average values of density and magnetization were used as initial parameters in the modeling process. In addition to physical property data, mapped surface geology was used to constrain the models at the earth's surface. For example, the geology of our model along profile AA' is based on a geologic cross-section by Graymer (2000a).

Modeling Results for Profiles A, B, and C

Geophysical modeling suggests a much greater horizontal and vertical extent of the San Leandro gabbro than previously reported (Graymer, 2000a). Modeling indicates that the gabbro extends from the westernmost exposures west of the Hayward Fault to the Chabot Fault on the east. The Chabot Fault appears to preferentially follow the eastern boundary of the San Leandro gabbro body. Because the maximum magnetic and gravity anomalies associated with the San Leandro gabbro are displaced from one another by about 6 km (compare Figs. 2 and 3), it appears that the gabbro may change physical properties by becoming more magnetic and less dense to the northwest. A change in the depth extent of the gabbro is not sufficient to account for the displacement of the observed maxima. Higher magnetizations and lower densities to the northwest suggest that the causative body may be more altered to the northwest (Figs 2 and 3). Modeling also suggests that the uppermost parts of the gabbro may be fractured or weathered, reflected in a lower model density for these parts of the gabbro (Fig 5).

Our models reveal that the San Leandro gabbro dips about 75^{o} to 80^{o} to the east and extends to a depth of about 6 to 8 km. Magnetic models also indicate that several moderately magnetic and probably ultramafic rock bodies occur west of the Hayward Fault Zone and below the offshore San Leandro basin (Fig. 5, -9 to –14 km). These smaller tabular bodies are probably serpentinite rather than gabbro because they do not have an associated gravity high. The magnetic signature of these features can be readily discerned on the magnetic map shown in Figure 3.

To validate the easterly-dip of the San Leandro gabbro body, a detailed sensitivity test was performed primarily using the magnetic data for three different starting models: a west-dipping, vertical, and an east-dipping gabbro body. Both the west-dipping and vertical starting gabbro model, the shape of which was allowed to change by computer-drive inversion, was immediately replaced by an east-dipping gabbro body. Moreover, inversion of the east-dipping gabbro body remained essentially the same, especially within the upper portions of the model to a depth of 6 km. At depths greater than about 6 km, the inversion process attempts to fit the long-wavelength part of the anomaly that is difficult to resolve. This ambiguity in the deeper parts of the models is treated with different tectonic scenarios described below.

The depth extent of the gabbro is poorly constrained and may vary from about 6 km to greater depths with little effect on the observed geophysical signature. This is schematically illustrated in Figure 6 where we consider the depth extent of three models of the San Leandro gabbro. A tabular San Leandro gabbro body detached from an oceanic basement layer (Fig. 6A) may be difficult to distinguish from a gabbro model attached to flat lying oceanic basement (Fig. 6B). However, model C (Fig. 6C) depicting a folded and possibly thrusted gabbro body extending to the Mt Diablo region, is unlikely because it would produce characteristically high-amplitude gravity and magnetic anomalies east of the Chabot fault, in an area devoid of significant geophysical anomalies (Figs. 2 and 3) and seismic tomography anomalies (Hole *et al.,* 2000).

In addition to the magnetic anomaly caused by the San Leandro gabbro, moderately magnetic basement rocks (Fig. 6, not shown in Fig. 5) are required at mid-crustal depths to fit the observed long-wavelength magnetic gradient that parallels the Hayward Fault. The gently sloping gradient caused by this feature can be seen in magnetic profile along AA' (Fig. 5) from about –10 to +15 km and is present on all three profiles. Although the magnetic anomaly associated with this feature may extend for some distance west of the Hayward Fault, the western extent of the causative body is equivocal because of the inherent limitations in the gravity and magnetic modeling and the uncertainty in its magnetic properties. Jachens and others (1995) discuss this feature in some detail and show that a magnetic source at a depth of about 16 km fits the observed anomaly best and that the western extent of this feature may intersect the Hayward Fault.

Discussion

Gravity data reveal that the Hayward Fault Zone is characterized by a steep isostatic gravity gradient whose symmetry is typical of a near vertical fault step, juxtaposing dense Franciscan basement on the southwest against lower-density Great Valley Sequence on the northeast (Fig. 2). This is particularly evident for the northern segment of the Hayward Fault Zone. A prominent positive gravity and magnetic anomaly along the Hayward Fault occurs in the immediate vicinity of San Leandro and near Hayward. The large amplitudes of these gravity and magnetic anomalies indicate that the associated rock is dense and magnetic compared to the surrounding rocks. Here we expand on these simple observations to define the 3D geometry of the San Leandro block (Fig. 6) which leads to hypotheses on its origin, its relation to earthquake occurrence, and the evolution of the Hayward Fault.

The amplitude of the gravity anomaly is about 14 mGal and is caused by a relatively dense gabbro body exposed in places along the trace of the Hayward Fault. Although the exposed gabbro varies from about 1/2 to 2 km in width, boundary analysis of gravity and magnetic data indicate that the body is about 3-km wide, even at shallow depths. These results are tightly constrained by the boundary analysis that is independent of the assumed physical properties of the gabbro body.

Geophysical data reveal little or no apparent offset of the San Leandro gabbro body along the Holocene trace of the Hayward Fault. Similarly, Graymer *et al.* (1995) found that identical lithic units on either side of the fault near Hayward only exhibit a few kilometers of offset on the recent trace of the Hayward Fault in contrast to the Chabot Fault where offset gravels exhibit apparent right-lateral displacement of about 23 km. Wakabayashi (1999a) indicated that in the northern Berkeley Hills, the main stratigraphic offset is up to about 1 km east of the recent trace of the Hayward Fault and that additional offsets may be present west of the recent trace of the Hayward Fault. Similar relationships are observed along the central part of the San Andreas Fault (Sims, 1993) and may be a characteristic feature of right-lateral strike-slip faults of the San Andreas Fault System (Wakabayashi, 1999a). This result is also supported by geologic evidence that indicates that a mapped gabbro block along the west side of the creeping strand of the Hayward Fault may have an offset of only about 5 km (e.g., Graymer, 2000a).

Geology and Seismicity

Seismicity data (Fig. 1) indicate an earthquake cluster in the vicinity of the San Leandro gabbro. Seismicity extends to a depth of 12 km, with the greatest concentration at depths between 3 and 9 km. The seismicity from the Northern California Seismic Net (NCSN) data (Fig. 1) yield results similar to hypocenters (Fig. 5) relocated using a high-resolution method to minimize residuals between observed and theoretical travel-time differences or double-differences (Waldhauser and Ellsworth, 2000; 2002). Relative locations between earthquakes are accurate to better than a few tens of meters while absolute location uncertainties are probably improved by an order of magnitude compared to catalog data (Waldhauser and Ellsworth, 2000; 2002). All magnitudes are displayed

for the relocated hypocenters, whereas the NCSN catalog data (Fig. 1) were thinned to eliminate poorly constrained data and magnitudes less than 1. No earthquakes greater than magnitude 4.0 have occurred in the immediate vicinity of the San Leandro gabbro since 1969 and most are magnitude 2.0-3.0. Seismicity correlates well with the independently and geophysically derived southwestern, lower bounding surface of the San Leandro gabbro (Fig. 5). Of particular importance is that most earthquake hypocenters are located outside the San Leandro gabbro.

There are at least two possible mechanical reasons for the correlation of hypocenters with the southwest edge of the San Leandro gabbro. The first is that stress may build up around the periphery of an igneous body much the same way that stress concentrates near knots in wood under an external stress. The stress concentration is proportional to the elastic rigidity contrast of the body and surrounding medium. A relationship between local stress accumulations and large igneous intrusions has previously been proposed (e.g., Kane, 1977; Long and Champion, 1977; McKeown, 1978; Hildenbrand *et al.*, 2001). Analytical solutions for stress concentrations near circular or elliptical intrusions were described by Donnel (1941) and Campbell (1978). Campbell (1978) calculated that if the inclusion has a higher rigidity modulus (is stiffer) than the surrounding rocks, the highest differential stress concentrations occur inside the inclusion and in small pockets just outside the inclusion. If the inclusion has a lower rigidity modulus than the surrounding rocks, the highest differential stress concentrations occur in small pockets just outside the inclusion. In any case, differential stress concentrations appear to be associated near inclusion boundaries.

A second explanation for the hypocenter locations is that they roughly outline the path of upward-propagating fault slip related to plate motion deep within the lithosphere, presumably following a pre-existing structure to accommodate slip. At a depth of roughly 10 km, the high strength of the San Leandro block would impede fault slip locally and tend to repel the upward slip encroachment. Thus, the block is nearly devoid of seismicity and represents the eastern boundary of the observed near-vertical pattern of hypocenters (Fig. 5).

At shallow depths (< 2 km), slip is comparatively aseismic and occurs within the geophysically defined San Leandro block, evidenced by the creeping recent trace of the Hayward Fault lying near the axis of the block. Here slip may follow a path of least resistance along several near-surface and possibly anastomosing faults within an upper zone of the block where the rocks are weak due to, for example, weathering, fracturing, or alteration. The maximum gravity high over the San Leandro gabbro is also coincident with a salient (or slight bend) along the recent trace of the Hayward Fault (Fig. 2), suggesting that the gabbroic block may also influence the trend of the recent trace of the Hayward Fault. Thus, the San Leandro gabbro body may represent a fault-zone discontinuity or segment boundary along the Hayward Fault.

An implication of the proposed fault model is that a zone of near-surface and anastomosing faults primarily accommodate slip in the upper parts of the San Leandro block, and at relatively shallow depths, they intersect the ancestral Hayward Fault, dipping roughly 75^{o}NE (Fig. 5). Fault slip propagating upwards along the main or ancestral Hayward Fault encounters a weak zone in the upper parts of the San Leandro gabbro, resulting in a change in the slip path along branches within the gabbro. We would thus expect that large stress accumulations occur at depth along the ancestral Hayward Fault (where the block may impede fault slip) and that the shallow observed creep and seismic slip are responses to this larger, deeper stressed volume. These interpretations suggest that major earthquakes in the vicinity of the San Leandro block would originate along the deeper portions of the recent trace of the Hayward Fault that coincide with the ancestral Hayward Fault.

The shape and extent of the San Leandro gabbro, its geologic relationships, and associated seismicity suggest that the Hayward Fault Zone evolved from a pre-existing feature, possibly an ancestral, low-angle roof thrust (e.g., Wentworth *et al.*, 1984) that ultimately brought relatively flat-

lying oceanic crust (e.g., Dickinson, 1981; Furlong, 1993; Brocher *et al.*, 1994) to the surface. We recognize that other mechanisms could have produced the pre-existing structure that the Hayward Fault preferentially followed, like attenuation-related faults or subduction-related thrusts. However, of these possible mechanisms, only a low-angle roof thrust mechanism requires a relatively flat-lying section of oceanic crust at depth that is indicated in the geophysical interpretations (Jachens *et al.*, 1995).

Conclusions

Because of the geophysical properties of mafic and ultramafic rocks and their occurrence along the Hayward Fault Zone, gravity and magnetic investigations afford us a unique opportunity to resolve the nature, spatial relationship, and evolution of the Hayward Fault Zone. Improved understanding of the three-dimensional geometry and physical properties of the Hayward Fault Zone will provide additional constraints on seismic hazard probability, earthquake modeling, and fault interactions that are applicable to other major strike-slip faults around the world.

Geophysical modeling indicates that the San Leandro gabbro is much more extensive in the subsurface than the outcrop pattern suggests. The gabbro body is tabular, dips steeply to the northeast, and extends to a depth of about 6 km or greater. The western boundary of the gabbro possibly represents the westernmost part of the Hayward Fault Zone and the eastern boundary of the gabbro coincides with the Chabot Fault.

The seismic cluster pattern along the southwest edge or lower bounding surface of the San Leandro gabbro and a salient in the recent trace of the Hayward Fault along the maximum gravity high associated with the gabbro suggest that the gabbro body plays an important role in the release of seismic energy. The western edge of the San Leandro gabbro probably defined a wedge or roof thrust that ultimately, after multiple episodes of extension and attenuation, evolved into the present near vertical fault. Thus, the three-dimensional geometry of the gabbroic body and its relation to earthquake seismicity suggest that the strike-slip Hayward Fault has preferentially followed a pre-existing feature.

The earthquake cluster at the southwestern edge of the San Leandro block at depths between about 3 and 9 km suggests that the block acts as an elastically stiff intrusion with stress build-ups around its periphery. This model might be tested by calculating perturbations to the stress field caused by the gabbro body. In addition, the model implies perturbations to the ambient strain field that might be compared to geodetic measurements and geologic deformation. Is it conceivable that this local stressed volume could be the nucleation or termination point of a new rupture related to a large earthquake? Although the answer to this question is enigmatic, the epicenter of the1868 earthquake, although poorly constrained, with an estimated Mw (Moment magnitude) of 7.0 (Yu and Segall, 1996) is in the region of the San Leandro block (Ellsworth, 1990; Bakun, 1999).

Acknowledgments

We would like to thank Russ Graymer, Steve Hickman, Bob McLaughlin, Diane Moore, Bob Simpson, Bill Stuart, Carl Wentworth, and the Hayward Fault Working Group of the USGS for valuable discussions and suggestions. Earlier versions of this paper benefited from reviews by Russ Graymer, Diane Moore, Bob Simpson, Bill Stuart, John Wakabayashi, and an anonymous reviewer. We are also grateful to the Associate Editor of BSSA, Roland Bürgmann for helpful comments and suggestions that greatly improved the manuscript.

References

Bailey, E.H., M.C. Blake, Jr., and D.L. Jones (1970). On-land Mesozoic oceanic crust in Californiia Coast Ranges, *U.S. Geol. Surv. Prof. Pap. 700-C*, C70-C81.

Bakun, W.H. (1999). Seismic activity of the San Francisco Bay region, *Bull. Seism. Soc. Am.* **89**, 764-784.

Baranov, V. (1957). A new method for interpretation of aeromagnetic maps, pseudo-gravimetric anomalies, *Geophysics* **22**, 359-383.

Blakely, R.J. (1995). *Potential Theory in Gravity and Magnetic Applications*, Cambridge University Press, 441 pp.

Blakely, R.J., and R.W. Simpson (1986). Approximating edges of source bodies from gravity or magnetic data, *Geophysics* **51**, 1494-1498.

Brocher, T.M., J., McCarthy, P.E. Hart, W.S. Holbrook, K.P. Furlong, T.V. McEvilly, J.A. Hole, and S.L. Klemperer (1994). Seismic evidence for a lower-crustal detachment beneath San Francisco Bay, California: *Science* **265**, 1436-1439.

Burch, S.B. (1968). Tectonic emplacement of the Burro Mountain ultramafic body, Santa Lucia Range, California, *Geol. Soc. Am. Bull.* **79**, 527-544.

Bürgmann, R.D., D. Schmidt, R.M. Nadeau, M. d'Alessio, E. Fielding, D. Manaker, T.V. McEvilly, and M.H. Murray (2000). Earthquake potential along the northern Hayward Fault, *Science* **289**, 1178-1182.

Campbell, D.L. (1978). Investigation of the stress-concentration mechanism for intraplate earthquakes, *Geophys. Res. Lett.* **5**, 477-479.

Coleman, R.G. (1971). Petrologic and geophysical nature of serpentinites, *Geol. Soc. Am. Bull.* **82**, 897-918.

Coleman, R.G. (2000). Prospecting for ophiolites along the California continental margin, *Geol. Soc. Am. Spec. Pap.* **349**, 351-364.

Dickinson, W.R. (1981). Plate tectonics and the continental margin of California, in *The geotectonic development of California*, Ernst, W.G. (Editor), Rubey Volume 1, Prentice-Hall, Inc., Englewood Cliffs, New Jersey, 1-28.

Dickinson, W.R., C.A. Hopson, and J.B. Saleeby (1996). Alternate origins of the Coast Range Ophiolite (California): Introduction and implications, *Geol. Soc. Am. Today* **6**, no. 2, 1-10.

Dobrin, M.B., and C.H. Savit (1988). *Introduction to Geophysical Prospecting* (4th ed.), New York, McGraw-Hill, 867 pp.

Donnell, L.H. (1941). Stress concentrations due to elliptical discontinuities in plates under edge forces, *Theordore von Karmon Anniv. Vol.*, Pasadena, 293-309.

DuBois, R.L. (1963). Remanent, induced, and total magnetism of a suite of serpentinite specimens from the Sierra Nevada, California, *J. Geophys. Res.* **68**, 267-278.

Ellsworth, W.L. (1990). Earthquake history, 1769-1989, in *The San Andreas fault system, Californi,a* Wallace, R.E. (Editor), *U.S. Geol. Surv. Prof. Pap. 1515*, 153-187.

Fox, K.F., Jr., R.J. Fleck, G.H. Curtis, and C.E. Meyer (1985). Implications of the northwestwardly younger age of volcanic rocks of west-central California, *Geol. Soc. Am. Bull.* **96**, 647-654.

Furlong, K.P. (1993). Thermal-rheologic evolution of the upper mantle and the development of the San Andreas fault system: *Tectonophysics* **223**, 149-164.

Godson, R.H., and D. Plouff (1988). BOUGUER version 1.0, a microcomputer gravity-terrain-correction program, *U.S. Geol. Surv. Open-File Rept. 88-644*.

Graham, S.A., C. McCloy, M. Hitzman, R. Ward, and R. Turner (1984). Basin evolution during change from convergent to transform continental margin in central California, *Am. Assoc. Petr. Bull.* **68**, no 3., 233-249.

Graymer, R. (1995). Geology of the southeast San Francisco Bay Area Hills, California, in *Recent geologic studies in the San Francisco Bay Area*, Sangines, E.M., D.W. Andersen, and A.B. Busing (Editors), *Soc. Econ. Paleo. and Min.* **76**, 115-124.

Graymer, R.W. (2000a). Geologic map and map database of the Oakland metropolitan area, Alameda, Contra Costa, and San Francisco Counties, California, *U.S. Geol. Surv. Misc. Field Studies Map MF-2342*.

Graymer, R.W. (2000b). Neogene development of the Hayward Fault Zone – a different perspective on an active strike-slip fault, *Tectonics*. (submitted).

Graymer, R.W, Jones, D.L., and Brabb, E.E., (1995). Is there more Quaternary displacement on the Chabot fault than on the Hayward fault?, *Am. Assoc. Petr. Geol. Bull.* **79**, 585.

Hildenbrand, T.G., W.D. Stuart, and P. Talwani (2001). Geologic structures related to the New Madrid earthquake near Memphis, Tennessee, based on gravity and magnetic interpretations: *Eng. Geol.*, 17 pp. (in press).

Hole, J.A., T.M. Brocher, S.L. Klemperer, T. Parsons, H.M. Benz, and K.P.Furlong (2000). Three-dimensional seismic velocity structure of the San Francisco Bay area, *J. Geophys. Res.* **105**, 13,859-13,874.

Hopson, C.A., Mattinson, J.M., and Pessagno, E.A., (1981). Coast Range ophiolite, western California, in *The geotectonic development of California*, Ernst, W.G. (Editor), Rubey Volume 1, Prentice-Hall, Inc., Englewood Cliffs, New Jersey, 419-510.

Hopson, C.A., E.A. Pessagno, Jr., J.M. Mattinson, B.P. Luyendyk , W. Beebe, D.M. Hull, I.M. Muñoz, C.D. Blome (1996). Coast Range Ophiolite as paleoequatorial mid-ocean lithosphere, *in* Dickinson, W.R., C.A. Hopson, and J.B. Saleeby, Alternate origins of the Coast Range Ophiolite (California): Introduction and implications, *Geol. Soc. Am. Today* **6**, no. 2, 4-6.

Jachens, R.C., A. Griscom, and C.W. Roberts (1995). Regional extent of Great Valley basement west of the Great Valley, California, Implications for extensive tectonic wedging in the California Coast Ranges, *J. Geophys. Res.* **100**, 112,769-12,790.

Jachens, R.C., and C.W. Roberts (1981). Documentation of a FORTRAN program, 'isocomp', for computing isostatic residual gravity, *U.S. Geol. Open-File Rept. 81-574*.

Jennings, C.W., R.G. Strand, and T.H. Rogers (1977). Geologic map of California, *Calif. Div. of Mines and Geol.*

Kane, M.F. (1977). Correlation of major eastern earthquake centers with mafic/ultramafic basement masses: *U.S. Geol. Surv. Prof. Pap. 1028-O*.

Langel, R.A. (1992). IGRF, 1991 revision, *EOS Trans. AGU* **73**, 182. [IGRF, International Geomagnetic Reference Field]

Lienert, B.R., and P.J. Wasilewski (1979). A magnetic study of the serpentinization process at Burro Mountain, California, *Earth Planet. Sc. Lett.* **43**, 406-416.

Lienkaemper, J.J. (1992). Map of recently active traces of the Hayward Fault, Alameda and Contra Costa Counties, California: U.S. Geol. Surv. Misc. Field Stud. Map, 1:24,000, *MF-2196*, 13 pp.

Lienkaemper, J.J., G. Borchardt, and M. Lisowski (1991). Historic creep rate and potential for seismic slip along the Hayward Fault, California, *J. Geophys. Res.* **96**, 18,261-18,283.

Lienkaemper, J.J., J.S. Galehouse, and R.W. Simpson (1997). Creep response of the Hayward Fault to stress changes caused by the Loma Prieta earthquake, *Science* **276**, 2014-2016.

Lienkaemper, J.J., J.S. Galehouse,, and R.W. Simpson (2001). Long-term monitoring of creep rate along the Hayward fault and evidence for a lasting creep response to 1989 Loma Prieta earthquake, Geophys. Res. Lett. **28**, 2265-2268.

Lisowski, M., J.C., Savage, and W.H. Prescott (1991). The velocity field along the San Andreas fault in central and southern California, J. Geophys. Res. **96** (B5), 8369-8389.

Long, L.T., and J.W. Champion Jr. (1977). Bouguer gravity map of the Summerville-Charleston, South Carolina, epicentral zone and tectonic implications, *U.S. Geol. Surv. Prof. Pap. 1028-K*.

Marlow, M.S., R.C. Jachens, P.E. Hart, P.R. Carlson, R.J. Anima, and J.R. Childs (1999). Development of San Leandro synform and neotectonics of the San Francisco Bay block, California, *Mar. and Petrol. Geol.* **16**, 431-442.

Mattinson, J.M., and Hopson, C.A., (1992). U/Pb ages of the Coast Range Ophiolite: A critical reevaluation based on new high-precision Pb/Pb ages, *Am. Assoc. Petr. Geol. Bull.* **76**, 425.

McKeown, F.A. (1978). Hypothesis, mini-earthquakes in the central and southeastern United States are casually related to mafic intrusiveive bodies, *U.S. Geol. Surv. J. Res.* **6**, 41-50.

McLaughlin, R.J., W.V. Sliter, D.H. Sorg, P.C. Russell, and A.M. Sarna-Wojcicki (1996). Large-scale right-slip displacement on the east San Francisco Bay region fault system, California, Implication for location of late Miocene to Pliocene Pacific plate boundary, *Tectonics* **15**, 1-18.

Parsons, T. (1998). Seismic-reflection evidence that the Hayward Fault extends into the lower crust of the San Francisco Bay area, California, *Bull. Seism. Soc. Am.* **88**, 1212-1223.

Ponce, D.A. (2001). Principal facts for gravity data along the Hayward Fault and vicinity, San Francisco Bay Area, northern California, *U.S. Geol. Surv. Open-File Rept. 01-124*, 25 pp.

Saad, A.H. (1969). Magnetic properties of ultramafic rocks from Red Mountain, California, *Geophysics* **34**, 974-987.

Savage, J.C., and M. Lisowski (1993). Inferred depth of creep on the Hayward Fault, central California, *J. Geophys. Res.* **98**, 787-793.

Simpson, R.W. (2000). Watching the Hayward Fault, *Science* **289**, 1147-1148.

Simpson, R.W., R.C. Jachens, R.J. Blakely, and R.W. Saltus (1986). A new isostatic residual gravity map of the conterminous United States with a discussion on the significance of isostatic residual gravity anomalies, *J. Geophys. Res.* **91**, 8348-8372.

Simpson, R.W., J.J. Lienkaemper, and J.S. Galehouse (2001). Variations in creep rate along the Hayward Fault, interpreted as changes in depth of creep, *Geophys. Res. Lett.* **28**, 2269-2272.

Sims, J.D. (1993). Chronology of displacements on the San Andreas Fault in central California: evidence of reversed positions of exotic rock bodies neat Parkfield, California, in Powell, R.E., R.J. Weldon II, and J.C. Matti (Editors), The San Andreas Fault System: Displacement, palinspastic recontruction and geologic evoltion, *Geol. Soc. Am. Mem.* **178**, 231-256

U.S. Geological Survey (1992). Aeromagnetic map of Livermore and vicinity, California, *U.S. Geol. Surv. Open-File Rept. 92-531*.

U.S. Geological Survey (1996). Aeromagnetic map of the central San Francisco Bay area, California, *U.S. Geol. Surv. Open File Rept. 96-530*.

Wakabayashi, J. (1999a). Distribution of displacement on and evolution of a young transform fault system: The northern San Andreas fault system, California, *Tectonics* **18**, 1245-1274.

Wakabayashi, J. (1999b). The Franciscan Complex, San Francisco Bay area: A record of subduction processes, *in* Wagner, D.L., and S.A. Graham (Editors), Geologic field trips in northern California, *Calif. Div. of Mines and Geol. Spec. Publ.* **119**, 1-21.

Wakabayashi, J. (1992). Nappes, tectonics of oblique plate convergence, and metamorphic evolution related to 140 million years of continuous subduction, Franciscan Complex, California, *J. Geol.* **100**, 19-40.

Waldhauser, F., and W.L. Ellsworth (2000). A double-difference earthquake location algorithm, Method and application to the northern Hayward Fault, *Bull. Seism. Soc. Am.* **90**, 1353-1368.

Waldhauser, F., and W.L. Ellsworth (2002). Fault structure and mechanics of the Hayward Fault, California, from double difference earthquake locations, *J. Geophys. Res.* **107** (B3), 10.1029/2000JB000084.

Webring, M.W. (1985). SAKI--A Fortran program for generalized linear inversion of gravity and magnetic profiles, *U.S. Geol. Surv. Open-File Rept. 85-122*, 104 pp.

Wentworth, C.M., M.C., Jr Blake,. D.L. Jones, A.W. Walter, and M.D. Zoback (1984). Tectonic wedging associated with emplacement of the Franciscan assemblage, California Coast Ranges, in *Franciscan geology of northern California*, Blake, M.C. Jr. (Editor), *Soc. Econ. Paleo. Min., Pacific Section* **43**, 163-173.

Working Group on California Earthquake Probabilities (1999). Earthquake probabilities in the San Francisco Bay region, 2000 to 2030 – A summary of findings, *U.S. Geol. Surv. Open-File Rept. 99-517*, 60 pp.

Yu, E., and P. Segall (1996). Slip in the 1868 Hayward earthquake from the analysis of historical triangulation data, *J. Geophys. Res.* **101**, 16,101-16,118.

U.S. Geological Survey
345 Middlefield Rd., MS 989
Menlo Park, California, 94025
ponce@usgs.gov
(D.A.P., T.G.H., R.C.J)

Table 1
Physical property measurements for selected rock types

Rock type	No. of samples	GD (g/cm^3)	SBD (g/cm^3)	DBD (g/cm^3)	Susc (10^{-3} cgs)	Q
Ophiolitic rocks						
Gabbro	17	2.91	2.88	2.86	1.17	0.1
Serpentinite	9	2.61	2.48	2.39	2.79	0.1
Quartz keratophyre	2	2.59	2.57	2.57	0.00	0.1
Volcanic rocks						
Basalt	11	2.74	2.67	2.62	0.33	---
Andesite	4	2.61	2.59	2.56	0.03	---
Sedimentary rocks						
Graywacke	6	2.62	2.58	2.55	0.04	---
Shale	5	2.57	2.53	2.50	0.01	---
Sandstone	21	2.56	2.44	2.35	0.06	---
Siltstone	5	2.57	2.40	2.29	0.01	---

DBD, dry bulk density; GD, grain density; SBD, saturated bulk density; Susc, susceptibility; Q, Koenigsberger ratio (ratio of remanent and induced magnetization).

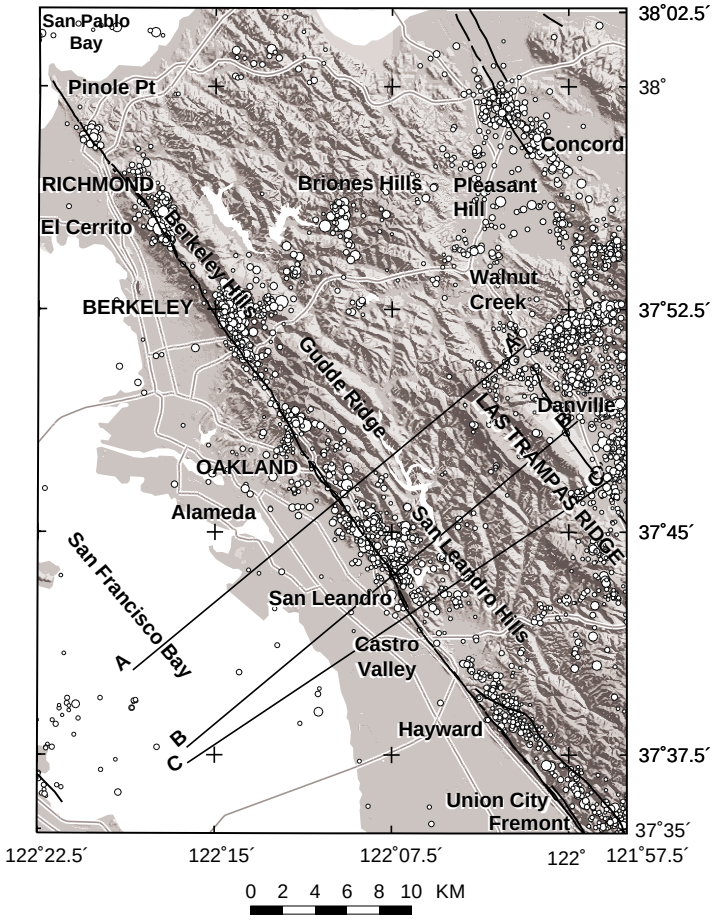

Figure 1. Shaded relief topographic map of the Hayward Fault Zone and vicinity showing seismicity (circles). Seismicity data are from the U.S. Geological Survey's Northern California Seismic Net (NCSN) catalog from 1969 through September, 23, 1999, M ≥ 1.0, P-wave arrivals ≥ 8, RMS travel-time residual ≤ 0.3 s, horizontal error ≤ 2.5 km, and vertical error ≤ 5.0 km. Circle, seismicity data (symbol size is proportional to earthquake magnitude); black lines; faults from Jennings et al. (1977) and recent trace of Hayward Fault from Lienkaemper et al. (1991). AA', BB', and CC', geophysical profiles.

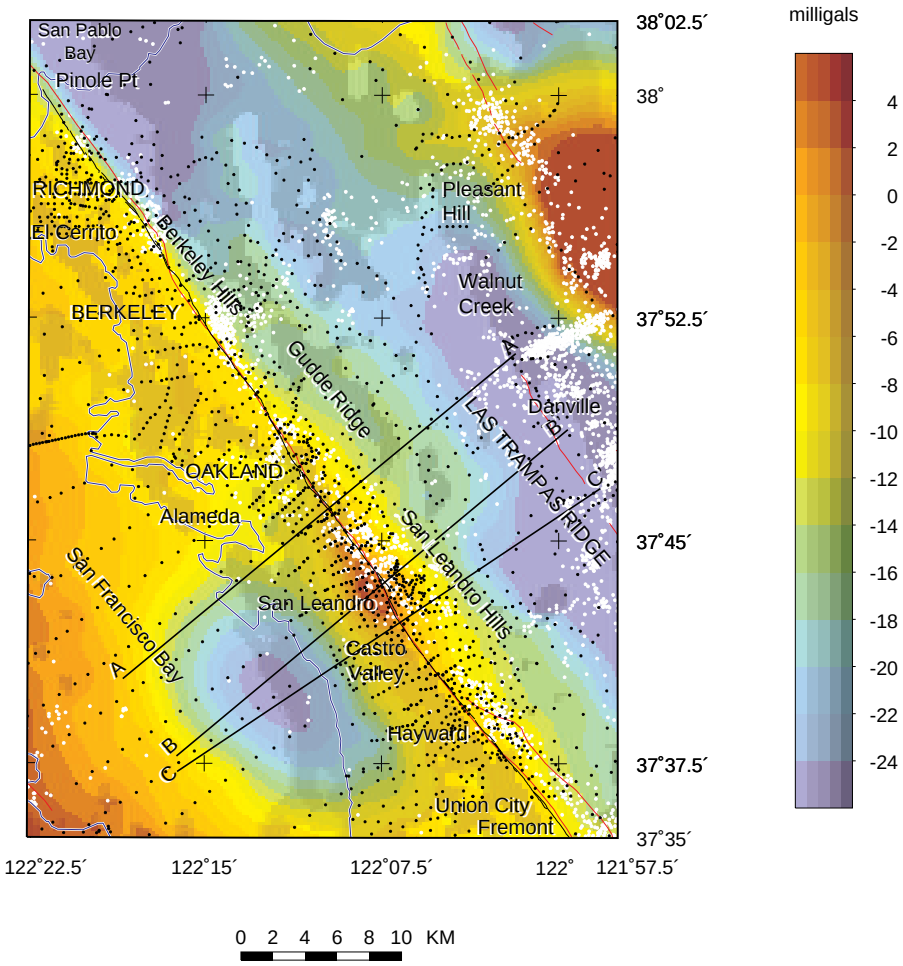

Figure 2. Isostatic gravity map of the Hayward Fault Zone and vicinity. Black triangles, gravity stations; red lines, faults from Jennings et al. (1977); black line, recent trace of Hayward Fault from Lienkaemper et al. (1991); white circles, seismicity as in Figure 1.

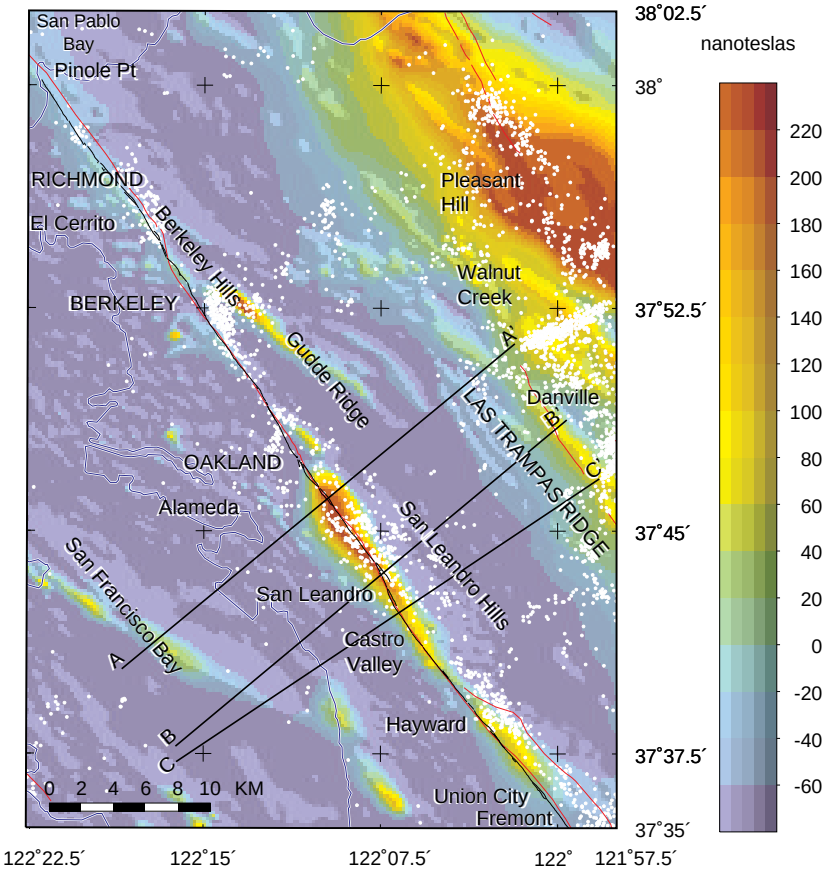

Figure 3A. Magnetic map of the Hayward Fault Zone and vicinity composed of two aeromagnetic surveys flown in a NE direction, with a flight-line spacing of 500 m (1/3-mi), and a nominal flight-line elevation of 250 m (820 ft) above water and 300 m (1,000 ft) above land. Explanation as in Figure 2.

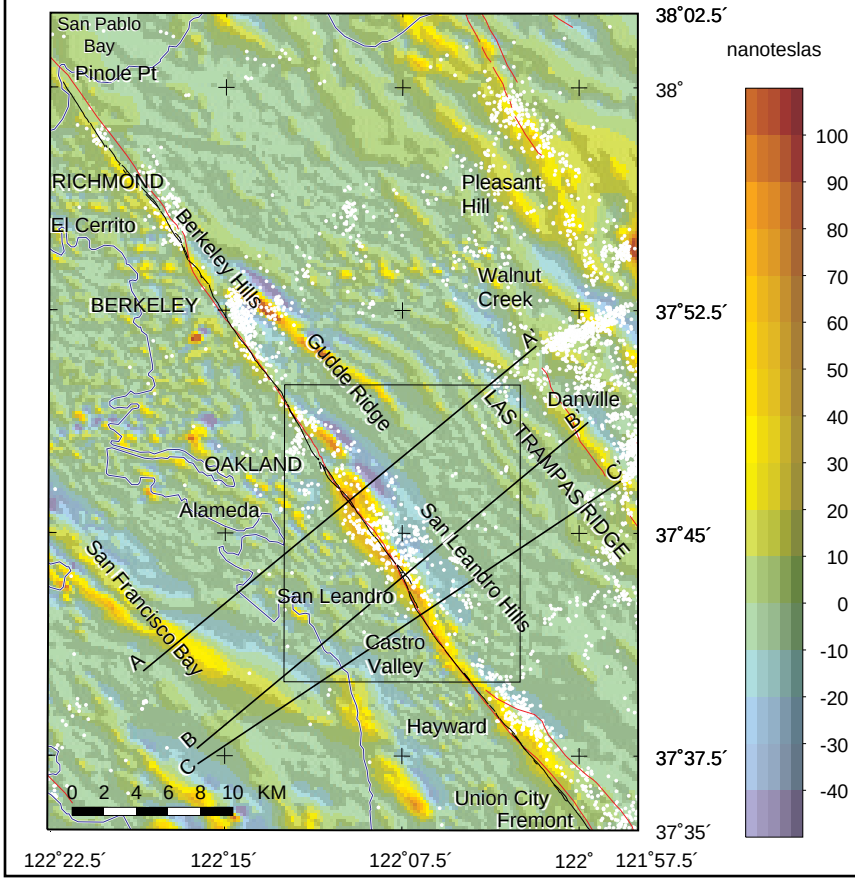

Figure 3B. Magnetic map enhancing shallow magnetic sources of the Hayward Fault Zone and vicinity. Shallow magnetic sources were enhanced by upward continuing the magnetic data a small distance (250 m) and then subtracting this field from the unfiltered data set to derive a residual field. The resulting map highlights magnetic sources within about 2.5 km of the surface. Explanation as in Figure 2. Expanded view of rectangular area is shown in Figure 4.

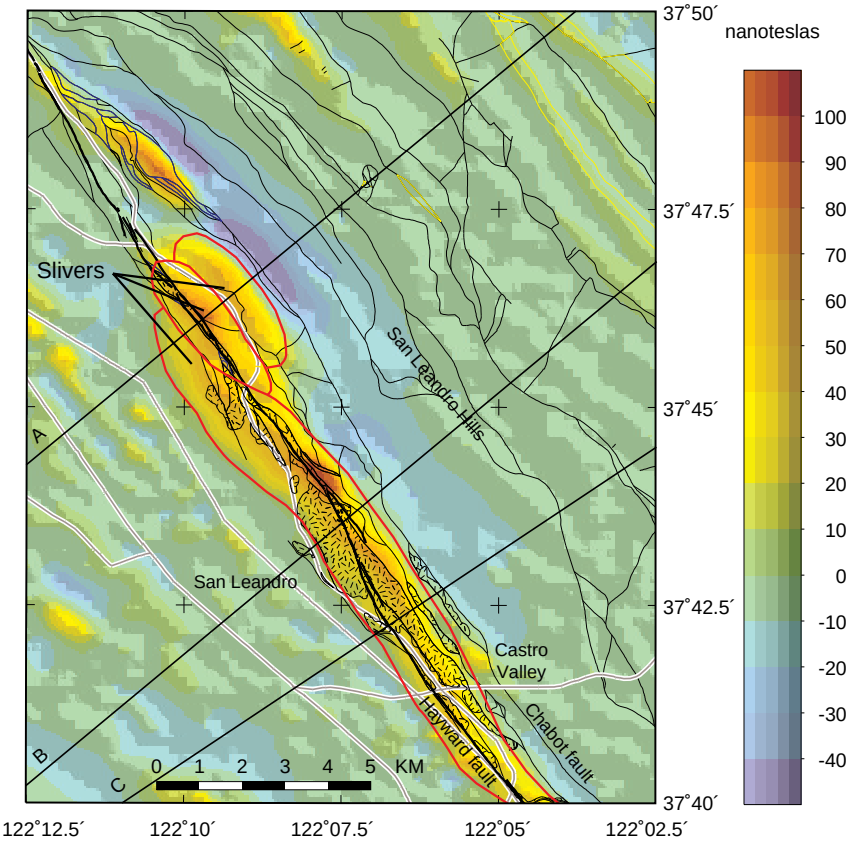

Figure 4A. Magnetic map enhancing shallow magnetic sources of the San Leandro gabbro and vicinity. Patterned area, San Lenadro gabbro; red outlines, gabbro slivers defined by magnetic anomalies. Explanation as in Figure 2. Geology modified from Graymer (2000a).

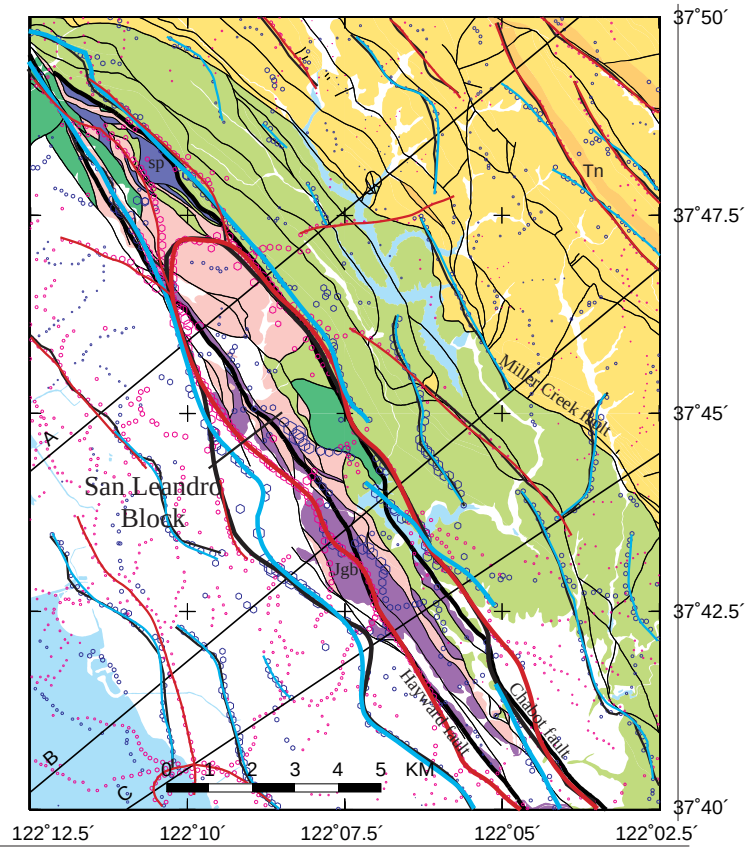

Figure 4B. Geophysical boundary of the San Leandro block and other geophysical lineaments defined by maximum horizontal gradients of gravity (blue) and magnetic (red) data. Bold blue and red lines define boundary of the San Leandro block. Geology modified from Graymer (2000a). Jgb (violet), gabbro; sp (blue), serpentinite; Tn (brown), Neroly Sandstone; black lines, faults. Bold black lines, recent trace of the Hayward and Chabot faults (Lienkaemper et al., 199; Graymer, 2000a). Eastern edge of San Leandro block correlates with the Chabot fault.

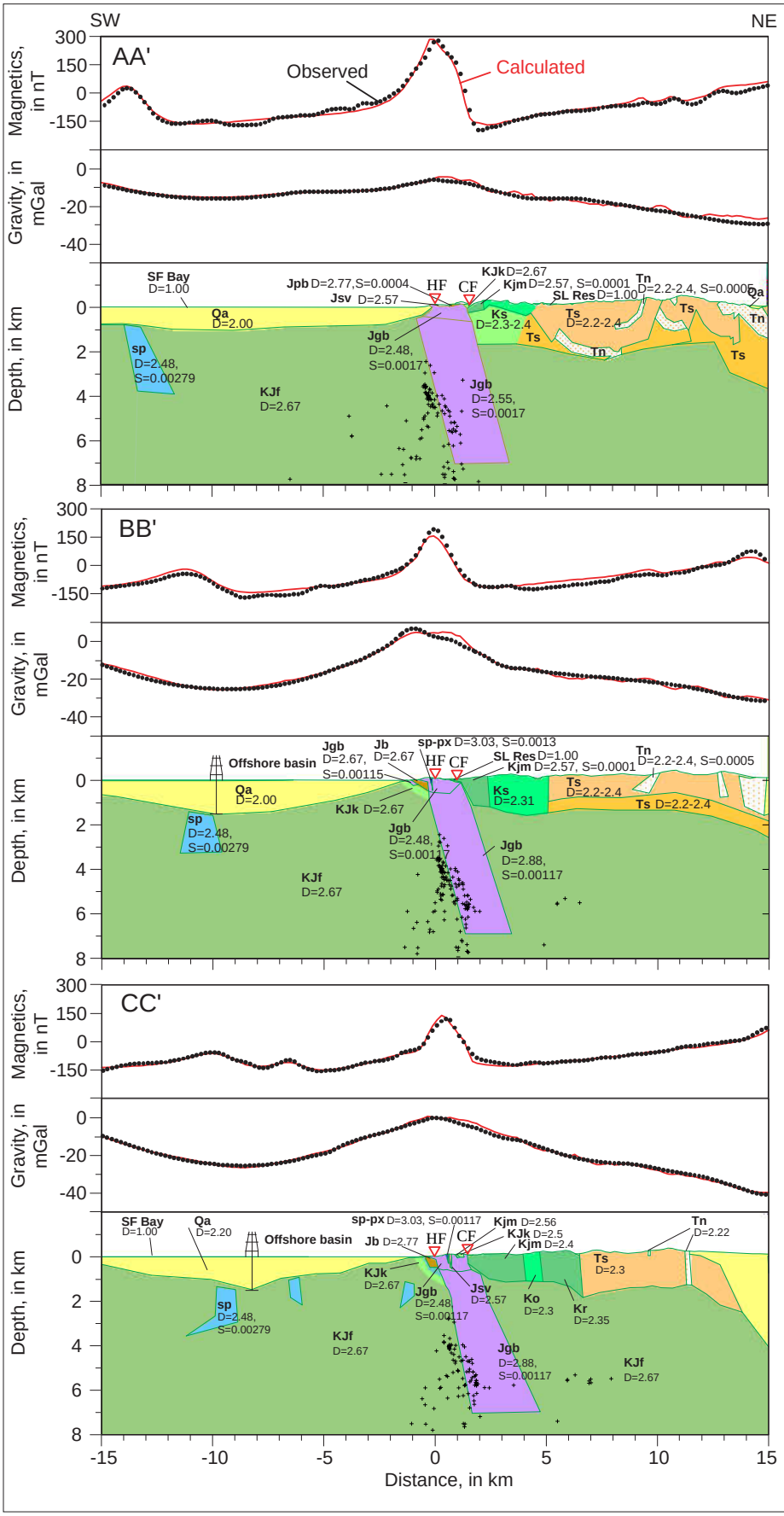

Figure 5. Gravity and magnetic models across the San Leandro gabbro. Physical properties are based on measurements on rocks and core samples (Table 1). Profile AA' is along and partly based on a geologic cross-section by Graymer (2000a). Profile BB' and CC' are based on surface geology by Graymer (2000a). Geologic symbols: Qa, Quaternary alluvium and related low-density materials; Tn, Neroly Sandstone; Ts, undifferentiated Tertiary sedimentary rocks; KJf, Franciscan Complex; Kjm, Joaquin Miller Formation; KJk, Knoxville Formation; Ko, Oakland Conglomerate; Ks, undifferentiated Cretaceous sedimentary rocks; Jb, basalt; Jgb, gabbro; Jpb, pillow basalt; Jsv, quartz keratophyre; sp, serpentinite; sp-px, pyoxenite. Geographic and other symbols: SF Bay, San Francisco Bay; SL Res, San Leandro Reservoir; Inverted red triangles, recent trace of Hayward Fault (HF) and Chabot Fault (CF); D, density in g/cm3; S, susceptibility in CGS units; Drill-hole symbol, thickness of offshore sedimentary basin from seismic and gravity data (Marlow et al., 1999); +, seismicity from relocated hypocenters using a high-resolution double difference relocation procedure within 5 km of the profile (Waldhauser and Ellsworth, 2000;2002). No vertical exaggeration.

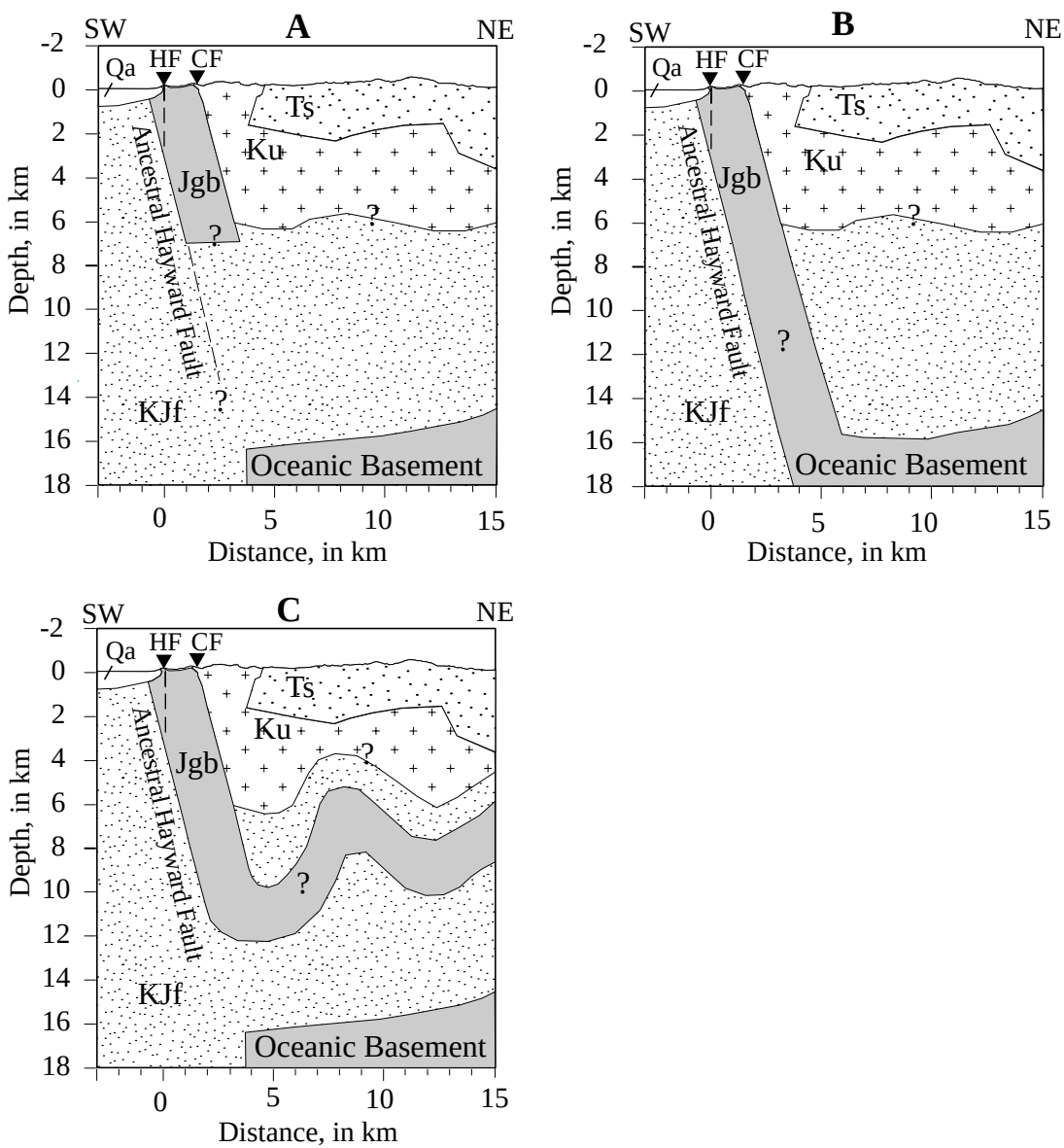

Figure 6. Schematic cross sections along profile AA' across the northern part of the San Leandro gabbro. A, model of a tabular San Leandro gabbro body detached from oceanic basement layer. B, model suggesting that the San Leandro gabbro is attached to flat lying oceanic basement. C, model with the San Leandro gabbro and coast range fault folded and thrusted and extending to the Mt Diablo region. Geophysical modeling may not be able to resolve the differences between model A and B, but model C is unlikely. Geologic symbols, Qa, Quaternary alluvium and related low-density materials; Ts, undifferentiated Tertiary sedimentary rocks; KJf, Franciscan Complex; Ku, undifferentiated Cretaceous Great Valley Complex; Jgb, gabbro. Inverted black triangles, recent trace of Hayward Fault (HF) and Chabot Fault (CF); ?, questionable boundary, other boundaries based on geologic information and geophysical modeling.